JOURNAL OF combinatorial CHEMISTRY

Article

Optimizing Photo-Embossed Gratings: A Gradient Library Approach

Berend-Jan de Gans, Carlos Snchez, Dimitri Kozodaev, Daan Wouters, Alexander Alexeev, Michael J. Escuti, Cees W. M. Bastiaansen, Dirk J. Broer, and Ulrich S. Schubert

J. Comb. Chem., **2006**, 8 (2), 228-236• DOI: 10.1021/cc0500506 • Publication Date (Web): 26 January 2006

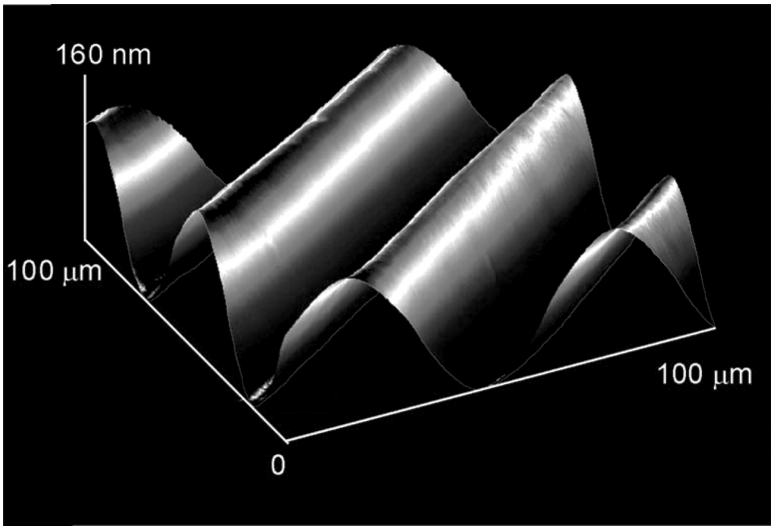

More About This Article

Additional resources and features associated with this article are available within the HTML version:

- Supporting Information
- Links to the 5 articles that cite this article, as of the time of this article download
- Access to high resolution figures
- Links to articles and content related to this article
- Copyright permission to reproduce figures and/or text from this article

View the Full Text HTML

Journal of Combinatorial Chemistry is published by the American Chemical Society.
1155 Sixteenth Street N.W., Washington, DC 20036

Optimizing Photo-Embossed Gratings: A Gradient Library Approach

Berend-Jan de Gans,[†] Carlos Sánchez,[‡] Dimitri Kozodaev,[†] Daan Wouters,[†] Alexander Alexeev,[†] Michael J. Escuti,[‡] Cees W. M. Bastiaansen,[‡] Dirk J. Broer,[‡] and Ulrich S. Schubert*[,†]

Laboratory of Macromolecular Chemistry and Nanoscience, and Polymers in Information and Communication Technology Group, Department of Chemical Engineering, Eindhoven University of Technology and Dutch Polymer Institute (DPI), PO Box 513, 5600 MB Eindhoven, The Netherlands

Received April 14, 2005

Methodologies for the rapid screening of coating systems were developed and applied to photopolymer lacquers for photoembossing applications. Continuous and discrete gradient libraries were prepared with a gradient in grating period along the short axis and along the long axis, a gradient in exposure energy, development temperature, film thickness, photoinitiator concentration, or monomer to polymer mass ratio. Discrete gradient libraries consisted of arrays of rectangular films made by pipetting a certain amount of sample onto a chemically patterned substrate consisting of hydrophilic patches surrounded by hydrophobic, fluorinated barriers. The shape and height of the photoembossed gratings were measured using an automated AFM. Optimum grating height was obtained for a 20-μm period at intermediate exposure energies, photoinitiator concentrations, or both. Height improves with development temperature (max 110 °C), monomer-to-polymer ratio (max 55 wt % monomer), and film thickness. Surface topography can also be optimized, depending on any specific application.

Introduction

Combinatorial materials research is a cyclic process that essentially comprises four steps: (1) Parallel preparation of materials, followed by (2) the fast preparation of sample libraries of these materials. The term library refers to a number of samples on a common substrate that are ordered such that they can be conveniently and rapidly characterized. (3) Analysis of the data follows characterization. The goal is to build a statistical model and to find the optimum composition, which is based on some performance criterion. (4) After that, the process should start from the beginning to validate the prediction of the model and further optimize the composition. The combinatorial approach promises an increase in the rate of discovery of new (polymeric) materials and the identification of quantitative structure−property relationships (QSPR), but can only be successful if all four steps are addressed sequentially. With the advent of automated facilities for synthesis, formulation, and characterization, the bottleneck in combinatorial materials research has shifted to sample preparation, most notably if the properties to be characterized, such as thermal, mechanical or optical properties, require a solid sample.

Most combinatorial studies in the field of polymer science concern polymer films and coatings. Here, two conceptually different approaches to library preparation can be discerned, i.e., continuous and discrete. Amis, Meredith et al. were the first to prepare continuous libraries by doctor-blading of polymer films with a continuous composition or thickness gradient.[1−4] They used a second thermal or surface energy gradient orthogonal to the first, resulting in a 2-dimensional library of phase behavior or wetting properties.

Continuous libraries have two major advantages. The first is the information density of the samples. Second, it is sometimes easier to prepare a continuous gradient than a discrete one, in particular, when temperature is involved. However, extending the continuous approach to a three- or more dimensional composition space is difficult. On the other hand, the variation of several compositional parameters using a discrete approach can easily be done. Another disadvantage of continuous libraries is the fact that compositional parameters that yield the best results are not known a priori but have to be determined in a separate experiment.

In the discrete approach, a number of different substances or formulations are prepared and deposited onto a common substrate to form a rectangular array of films of known composition. The size of these films typically ranges from 10 to 1000 mm^2. It is a major challenge to prepare arrays of films that are flat and homogeneous. Arrays of layered structures consisting of small molecules have been prepared by vapor deposition in combination with clever masking strategies.[5] High-molecular-weight species, such as polymers, however, must be deposited from solution. This imposes a new problem, because a drying film usually produces a ring stain that contains almost all of the solute.[6] It has been shown that using a centrifuge, ring formation can be overcome when the substrate dries in a gravitational field.[7,8] Another strategy is to use mixtures of low- and high-boiling solvents.[9] In addition, the deposited solution should be confined in some way to prevent excessive spreading and mutual contamination. Another advantage of confinement is that by variation

* To whom correspondence should be addressed. Fax: 0031 40 247 4186. E-mail: u.s.schubert@tue.nl.
[†] Laboratory of Macromolecular Chemistry and Nanoscience.
[‡] Polymers in Information and Communication Technology Group.

10.1021/cc0500506 CCC: $33.50
Published on Web 01/26/2006

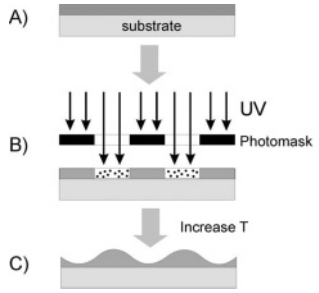

Figure 1. The principle of photoembossing. A film is casted on some substrate (A). It is then exposed to UV radiation using a photomask, thereby forming a latent image of free radicals entrapped in the polymer matrix (B). By heating the sample, the monomer locally polymerizes, resulting in a diffusive flux of unreacted monomer toward the exposed regions and a relief structure.

of the deposited amount of solution, the thickness of the obtained film can be varied in a controlled way. Confinement can be mechanical by using a hole-containing template.[7,8,10] Another very promising approach is to use a chemically patterned substrate. Here, the hydrophobic surface has an array of wettable, hydrophilic regions. Solutions are deposited on the hydrophilic regions and spread until the hydrophobic border is reached. In the approach of Boussie and Devenney, the substrate is rendered hydrophobic through coating with organosilanes.[11,12] In addition, the substrate has several regions that are covered with a thin film of a nonsilanizable material, typically gold. The polymer solutions are then deposited on the gold patches prior to characterization.

In this paper, we describe the preparation of both discrete and continuous libraries to improve the performance of photoembossed coatings. Photoembossing is a new, versatile, and simple technique (as compared to classical photolithography) for the large-scale, large-area production of well-defined relief structures in thin polymer films.[13−16] Such structures have a very large impact in different branches of technology and find application as light-controlling reflectors in display devices or traffic signs, or they can be part of biosensors and cell growth arrays,[17,18] microelectronic, and micro-optical elements.[19,20] A lacquer used for the purpose of photoembossing typically consists of a multifunctional acrylate, a photoinitiator, and a polymeric binder. A latent image of free radicals forms upon illumination at room temperature through a suitable mask. The lacquer must be glassy at room temperature to inhibit diffusion of radicals and polymerization at this stage. In addition, contact masking can be used without any deterioration of the lacquer. The relief structure forms upon heating above the glass transition of the lacquer. Polymerization occurs selectively in the exposed regions. The consumption of monomer leads to a net flux of unreacted monomer from the nonexposed to the exposed regions. This swells the exposed regions and results in a relief structure. The process is shown schematically in Figure 1.

The outcome of the photoembossing process depends on a large number of parameters, for example, the chemical nature of the monomer, polymer, photoinitiator, and potential additives; their respective concentrations; period of the relief structure; exposure energy; development temperature; and thickness of the film. Here, we describe a set of combinatorial experiments to study the influence of some of these parameters on the relief structure. We introduce new convenient methodologies for the preparation of 2-dimensional libraries, both continuous and discrete, that do not depend on any specific physical or chemical properties and that can easily be applied to other coating systems, as well. Using these new techniques, we prepared a series of 2-dimensional gradient libraries, each with a gradient in grating period along the one axis and a gradient in exposure energy, development temperature, thickness, photoinitiator concentration, and monomer-to-binder ratio along the other. We have limited our compositional studies to change the concentration of the different components of our blend; however, our combinatorial methodology can easily be extended to other compositions by changing the type of polymer binder, monomer, photoinitiator or other additives as inhibitors, chain transfer agents, and others. We aim to obtain new insights into the photoembossing grating formation process. As pointed out above, these periodic structures can be used as light-controlling elements in certain display devices whose diffractive properties are determined by the height and shape of the relief structures. We shall show that our combinatorial approach allows us to identify conditions for the formation of an optimum grating. In addition, we want to demonstrate that the large body of experimental data that is generated makes this combinatorial methodology a valuable tool in the study of any physicochemical phenomena.

Last, we want to point out a general advantage of 2-dimensional discrete libraries. Because more than two parameters are varied at a time, cross-correlations with other parameters could be discovered. To this end, we work on a designed experiment, the results of which will be published in a separate paper[21] (see also ref 22 for a related publication).

Experimental Section

Materials. Polybenzyl methacrylate (M_w 70 kD; Scientific Polymer Products) was used as the binder, dipentaerythritol penta/hexa acrylate (Sigma-Aldrich, Steinheim, Germany) as a multifunctional monomer, and Irgacure 369 (Ciba) as the photoinitiator. Propylene glycol methyl ether acetate (Sigma-Aldrich, Steinheim, Germany), ethoxypropyl acetate (Alfa Aesar, Hexsham, UK), isopropyl acetate (Acros Organics, Geel, Belgium), and methylbenzoate (Fluka Chemika, Buchs, Switzerland) were used as solvents. Solutions of monomer, binder, and initiator either in a 50/50% w/w propylene glycol methyl ether acetate/ethoxypropyl acetate (for the continuous libraries) or in a 90/10% w/w mixture of isopropyl acetate/methylbenzoate (for the discrete libraries) were prepared by gentle stirring. In the past, it was shown that the latter solvent mixture is particularly effective in suppressing ring formation.[9] All solutions based on the isopropyl acetate/methylbenzoate mixture contained 33.0 wt % solid material (monomer + binder + photoinitiator). All solutions based on the isopropyl acetate/methylbenzoate mixture contained 4.0 wt % solid material. Solutions were filtered through 5-μm PTFE filters (Schleicher & Schuell, Dassel, Germany) before use.

Substrates. Continuous libraries were prepared on D263 glass plates, thickness 1.1 mm and 15.2 cm × 15.2 cm in

size. After cleaning with a sponge and detergent (Teepol, Orpington, UK), glass plates were subsequently refluxed with 2-propanol; ultrasonicated at 65 °C in demineralized water for 10 min; and finally, dried in an oven at 80 °C.

Discrete libraries were prepared using D263 glass plates, thickness 1.1 mm and 12.7 cm × 3 cm in size. The size of the glass plates was set by the size of the lithographic masks that will be discussed later. Glass plates were cleaned as follows. They were ultrasonicated in acetone for 5 min, rubbed with sodium dodecyl sulfate solution, ultrasonicated in sodium dodecyl sulfate solution for 5 min, flushed with demineralized water to remove the soap, ultrasonicated in 2-propanol, dried with an air flow, and subsequently treated in a UV−ozone reactor (PR-100, UVP, Upland, CA) for 30 min to remove any remaining organic contamination.

Immediately after cleaning and before discrete library preparation, the glass plates were chemically patterned. To generate this pattern, the glass plates were spin-coated with a layer of NFR-016D4 negative photoresist (JSR, Tokyo, Japan) at 1000 rpm for 120 s using an RC8 spin-coater (Süss Microtec, Garching, Germany). The photoresist was dried on a hotplate at 90 °C for 120 s and exposed to broadband UV light (Philips) for 5 min (lamp−sample distance, 30 cm), using a homemade steel mask. The sample was subsequently baked at 90 °C for 5 min and, finally, developed using TMA-238WA developer (JSR, Tokyo, Japan). The substrate was cleaned thoroughly by flushing with demineralized water and subsequently treated in the UV−ozone reactor for 30 min. The substrate was then coated with (tridecafluoro-1,1,2,2-tetrahydrooctyl)trichlorosilane (ABCR, Karlsruhe, Germany).[23] The UV−ozone treatment in this case replaces the treatment with the oxygen plasma. In a final step, the cross-linked photoresist was removed with acetone using ultrasonication. On each of the substrates prepared in this manner, 11 × 4 samples can be deposited. The dried films have a size of 8.5 × 4.3 mm.

Library Preparation. All libraries were prepared under Class 100 clean-room conditions. Continuous libraries were prepared by spin-coating using the RC8 spin-coater at 1000 rpm for 60 s (acceleration 200 rpm s^{-1}). Films with a thickness of 2.6 μm were formed. Discrete libraries were prepared by manual deposition of small amounts of solution (3−13 μL) onto the chemically patterned substrate using a pipet (Brand Transferpette, Wertheim, Germany) and allowed to dry under ambient conditions. This methodology does not depend on the nature of the photopolymer lacquer and can, in principle, be adapted to other systems, as well. Film thicknesses were measured using a Dektak 3M stylus profiler (Veeco, Woodbury, NY).

Grating Formation. A USHIO lithographic system (filter at 365 nm) was used to generate the gratings in combination with a rectangular lithographic mask (101 × 20 mm) that was divided into four sectors (101 × 5 mm). Each sector has a line grating with a periodicities of 40, 20, 10, and 5 μm, respectively (dark and transparent areas of the same size). This kind of mask allows generation of diffraction gratings of potential interest as optical elements. The power reaching the sample was 5 mW cm^{-2}. After exposure, the gratings were developed on a hotplate at 80 °C during 10 min. Finally, to fix the surface relief structure, the samples were flood-exposed for 10 min and heated to 80 °C for an additional 10 min. This step has negligible influence in the final relief structure.

To generate a discrete gradient in exposure energy dose, a rectangular, linearly variable neutral density filter (101 × 25 mm), divided into 11 sectors (9 × 25 mm) was used, with the optical density (OD) increasing from 0.04 (no absorption) to 2 in steps of 0.2. Alternatively, a temperature gradient heating stage (Leica VM HB) was used to investigate the effect of the development temperature. The temperature of the stage ranges from 50 to 260 °C over a distance of 30 cm, corresponding to a temperature gradient of 7 °C cm^{-1}. The size of our samples is 101 mm, corresponding to a temperature difference of approximately 70 °C over the entire sample.

Topography Characterization. We used an atomic force microscope (Solver LS, NT-MDT, Russia) for characterization. The instrument has an automated Yθ-stage for positioning. The accessible workspace is circular with a diameter of 15 cm. The maximum scan size is 100 × 100 × 10 μm. In addition, the Solver LS has an integrated optical system with 1.5-μm resolution. Cantilevers with a spring constant of 5.5 N m^{-1} (NSG01, NT-MDT, Russia) were utilized. All measurements were performed in tapping mode.

To improve the quality of the data, we performed four maximum-sized scans per film, yielding a total of 44 × 4 = 176 scans per library. Scans were situated at the edges of a 1 × 1 mm square in the middle of the film. To reduce the effect of scanner nonlinearity, the measuring time per scan was at least 3 min, the total measuring time per library, therefore, almost 9 h. The roughness was analyzed with the aid of integrated software tools based on the set of statistics equations according to ISO4287/1 standard.

Thermal Characterization. DSC traces were measured on a high-throughput automated Phoenix DSC204 F1 differential scanning calorimeter (Netzsch, Selb, Germany). The temperature ranged from 30 to 150 °C; the heating rate was 10 K min^{-1}. An empty aluminum sample holder was used as reference. Prior to characterization, samples were subsequently dried on a hotplate for 20 min at 80 °C and illuminated with a high-intensity UV illuminator (Oriel, Stratford, CT) for 10 min.

Results and Discussion: Continuous Libraries

Energy Dose−Grating Period ibrary. A precursor layer consisting of 47.5 wt % polybenzyl methacrylate as binder, 47.5 wt % dipentaerythritol penta/hexaacrylate as multifunctional monomer, and an additional 5 wt % of photoinitiator was spin-coated from propylene glycol methyl ether acetate/ethoxypropyl acetate solution. A library with a discrete gradient in grating periodicity (Λ) along the short axis and a discrete gradient in energy exposure dose (E) along the long axis was prepared by simultaneous exposure through the grating mask and the variable density filter, as shown in Figure 2.

To determine both height and shape, the relief structures were characterized by automated AFM measurements. Figure 3 shows some typical results. It is seen that in the case of the 5-, 10-, and 20-μm grating structures, the shape of the

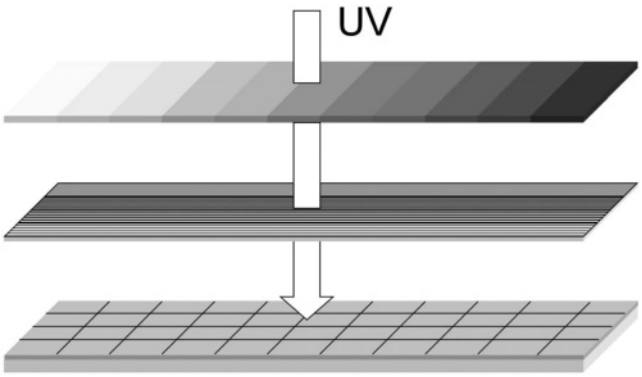

Figure 2. An energy dose−grating period library is formed by illumination with UV radiation through a gray scale mask and a grating mask simultaneously. A library of 44 different samples is, thus, prepared in one single step.

relief structure resembles a sinusoid. In the case of the 40-μm grating structure, a higher-order modulation appears: The sinusoidal shape is distorted by two extra upcoming peaks near the edges of the exposed regions. We shall come back to this point later. Some of the gratings efficiently diffract light, showing their potential as optical elements. Figure 4 shows the grating height as a function of energy dose and grating period. We defined the grating height as the difference in height between the irradiated and the dark areas.

Unlike relief height, quantitative representation of the changing shape of the photoembossed structures is not straightforward. In an attempt to assign a scalar measure to the shape of the relief structure, we applied Fourier analysis that leads to a parameter, S, that varies between 1 and −1 and that is independent of the relief height or grating period. First, we processed the two-dimensional AFM data (as in Figure 3, left column) in such a way as to produce an average one-dimensional surface curve $f(x)$ (similar to Figure 3, right column). Second, we determined the first few Fourier

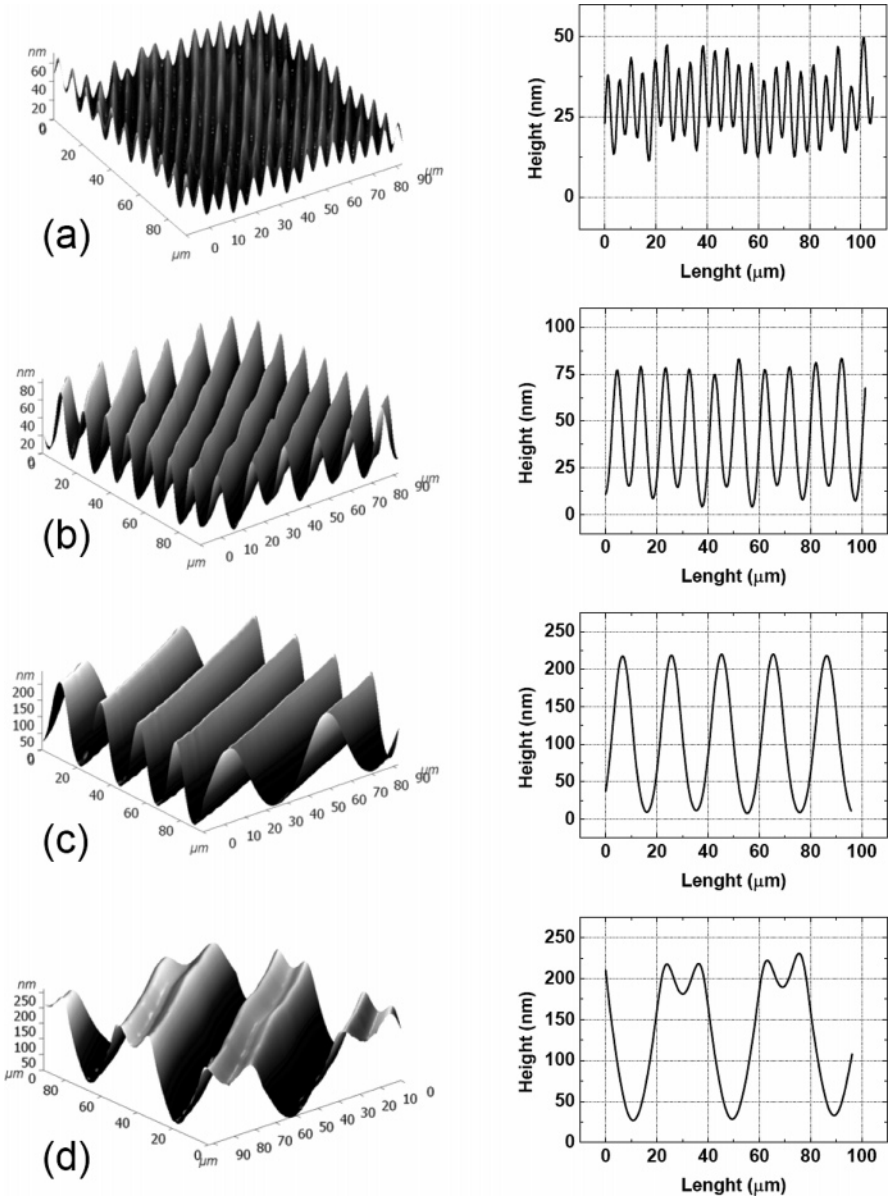

Figure 3. Relief structures with various grating periods formed by photoembossing of a sample containing 50% w/w polybenzyl methacrylate, 50% w/w dipentaerythritol pentaacrylate as multifunctional monomer, and an extra 5% w/w of photoinitiator. Grating period: (a) 5, (b) 10, (c) 20, and (d) 40 μm. Shown are a quasi-3D image and a cross section.

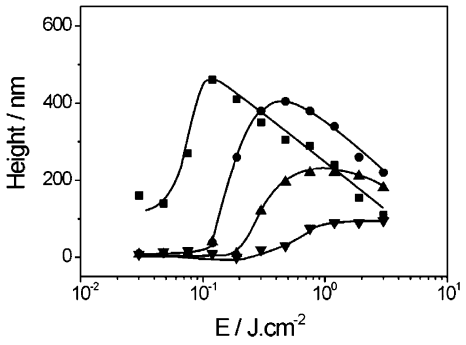

Figure 4. Grating height of exposure energy dose (E)−grating period library. Grating period: ■, 40; ●, 20; ▲, 10; and ▼, 5 μm. Lines are drawn to guide the eye.

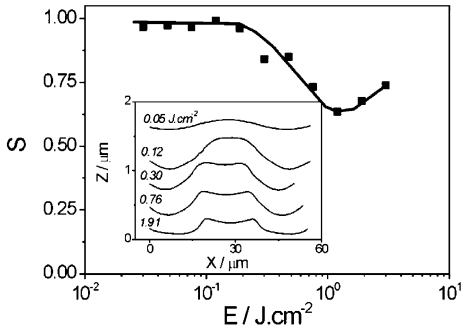

Figure 5. Shape-factors corresponding to the data shown in Figure 4. Grating period is 40 μm. The inset shows typical cross-sections with energy dose increasing from top to bottom.

series coefficients, $a_m = \Lambda^{-1} \int f(x)\, e^{-(i2\pi mx/\Lambda)}\, dx$ (where the integral occurs over one period). Finally, we compute a shape factor (S), defined as

$$S = \frac{|a_1|^2 - \sum_{n=2}^{M} |a_n|^2}{\sum_{n=1}^{M} |a_n|^2} \qquad (1)$$

where M is the maximum number of coefficients used for the calculation (in practice, we let $M = 5$, since the higher Fourier terms were nearly 0 for all the topologies of our samples). This shape factor S was inspired by the Michelson contrast,[24] used in image processing and information displays, and has the following properties: surface relief profiles similar to a sinusoid will lead to a value close to +1, whereas a decrease with respect to this value indicates deviation of the shape from a sinusoid, typically associated with the appearance of the shoulders at the edge of the relief plateaus (which are higher-order spatial frequencies).

As said above, the energy dose also influences the shape of the relief structure. The inset of Figure 5 shows typical cross sections of the relief structures obtained with a 40-μm grating mask. We observe the following trend: At low energy doses, we have a sinusoidal profile of small height that grows with energy dose. Eventually, shoulders begin to appear near the edges of the irradiated areas, and the height decreases. This is captured by our S parameter. Results of the shape analysis of the 40-μm gratings are shown in Figure 5. Up to energy doses of 0.2 J cm^{-2}, S is close to +1. Notice that the maximum height occurs at the upper end of this range (for 40-μm gratings). At higher energy doses, S decreases, indicating deviation from a sinusoidal profile and corresponding to the appearance of shoulders at the edges of the irradiated areas. We also notice that the decrease in S closely corresponds to the decrease in height. After this decrease of the shape factor S, it slightly increases again. It seems that the side shoulders, although clearly visible, decrease proportionally more than the central part of the hills (decrease in height), making S increase slightly. From this, we infer that shape imperfections do not occur for the 5- and the 10-μm gratings, with S close to +1 for the range of energies under study, and only up to a limited extent for the 20-μm gratings.

The results that are shown in Figures 3−5 can be explained with the help of Leewis' diffusion−polymerization model[25−27] that combines the effects of a polymerization-induced monomer concentration gradient with different mobilities of the binder and monomer, degree of cross-linking, interaction between the different components, and surface free energy. At room temperature, the polymer binder matrix immobilizes both the monomer molecules and the radicals generated during exposure. Heat increases mobility, and polymerization starts selectively in the exposed regions, generating a gradient in composition. A diffusion flux of unreacted monomer swells the exposed regions, resulting in a relief structure. At low energy doses, the height is quite small—typically below 100 nm—because only part of the photoinitiator molecules are activated. With increasing energy dose, the concentration of radicals and, thus, the height increase. In this energy dose range, cross-linking does not hinder monomer diffusion, and surface tension dictates a nearly sinusoidal profile. Eventually, a maximum is reached, which increases with grating period (at least in the range of periods under study). This is due to surface tension effects, because for a given size, the total surface of a sinusoidal relief structure increases with the height of the structure, h, and decreases with the period, Λ.

In the case of the 20- and the 40-μm gratings, the height decreases again with exposure dose after attaining a maximum. This phenomenon is known as overexposure: Excessive cross-linking of the overexposed regions inhibits diffusion of unreacted monomer toward the center of the exposed regions. Instead, monomer accumulates near the edges of the exposed regions, resulting in the higher order modulation that was described above. The effect is particularly pronounced for 40-μm gratings. Thus, the height at 40 μm is usually smaller than at 20 μm, despite surface energy. At smaller grating periods, the modulation appears at higher energy doses, as compared to the 40-μm case, or vanishes completely. This is due to the smaller diffusion lengths and the steeper monomer concentration gradient.

Our methodology is not limited to the kind of lithographic mask used in this study (useful to produce efficient gratings), but other types of gratings could be used either looking for other diffractive elements or to further explore the diffusion−polymerization properties of the photopolymer system. Thus, Leewis has studied theformation of saw-tooth-type relief gratings using gray-scale periodic masks.[25] We could also

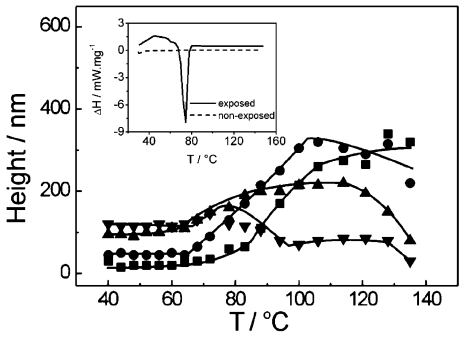

Figure 6. Grating height of development temperature (T)−grating period library. Grating period: ■, 40; ●, 20; ▲, 10; and ▼, 5 μm. Lines are drawn to guide the eye. Inset: DSC traces of exposed and nonexposed photopolymer lacquers. The exothermal peak of the exposed lacquer corresponds to polymerization of the acrylate monomer.

explore very wide periods (well above the typical diffusion lengths) to try to simulate a simple shadow edge. This would simplify the boundary conditions of the modeling (instead of periodic boundary conditions), since we would have an effectively infinite supply of monomer on the unexposed areas and an effectively infinite sink on the exposed side.

Development Temperature−Grating Period Library. Again, a lacquer consisting of 47.5 wt % polybenzyl methacrylate as binder, 47.5 wt % dipentaerythritol penta/hexaacrylate as multifunctional monomer, and an extra 5% w/w of photoinitiator was studied. A two-dimensional library with a discrete gradient in grating periodicity (Λ) along the short axis and a continuous gradient in development temperature (T) along the long axis was prepared using a temperature gradient heating stage. Within two libraries placed next to each other, the curing temperature varied from 50 to 135 °C.

Figure 6 shows the grating heights. For the 20- and the 40-μm period gratings, they initially remain constant but increase strongly above a critical temperature of ~70 °C. This is expected, because the mobility of the monomer increases with temperature. At very high temperatures, however, the grating height often decreases again, in particular, for smaller periods (5 μm). This may be due to a number of reasons, for example, an increased rate of the termination reaction. The inset of Figure 6 shows DSC traces of the sample. The exothermal peak originates from the polymerization reaction. Its onset at 69 °C closely corresponds to the temperature at which the grating height starts to increase. From the featureless DSC trace of the nonilluminated sample, we conclude that grating formation starts when the monomer mobility reaches a certain critical value without being related to a glass-transition.

Shape factors were calculated according to eq 1. Results of the analysis of the 40-μm gratings are shown in Figure 7. Low development temperatures result in high peaks near the edges of the exposed regions, corresponding to S-factors close to −1. The near-edge peaks gradually diminish with increasing temperature and mobility.

Results and Discussion: Discrete Libraries

Film Formation. Figure 8 shows a photograph of a typical substrate with 44 films. Such a substrate can be prepared in

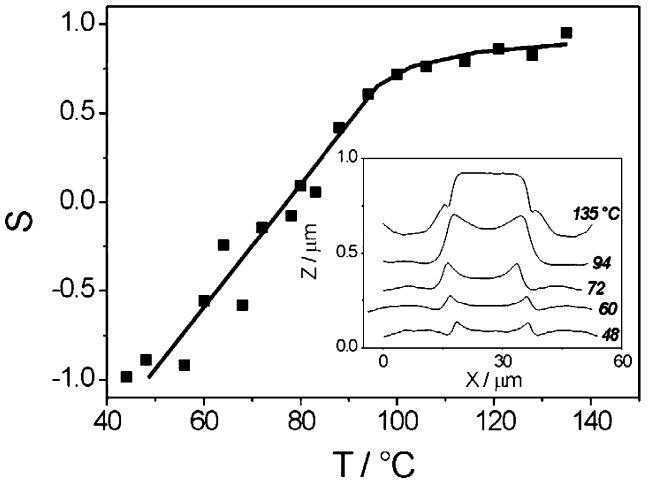

Figure 7. Shape factors corresponding to the data shown in Figure 6. Grating period is 40 μm. The inset shows typical cross sections with development temperature decreasing from top to bottom.

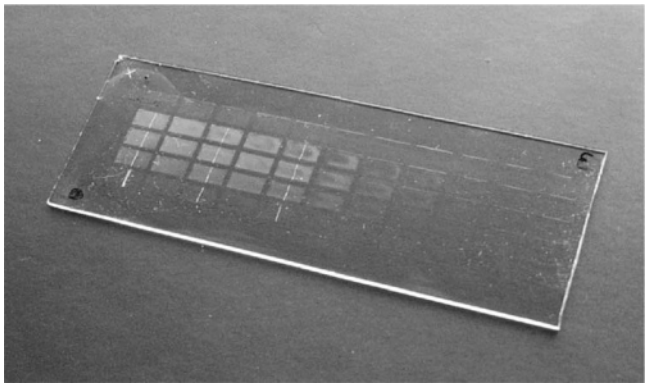

Figure 8. Photograph of a substrate with 44 samples.

<10 min. Sometimes films suffer from contact line depinning: During the drying process, the contact line of the film does not remain fixed, but instead retracts to form a film with ill-defined thickness. If film thickness influences the process of relief structure formation—and we shall see that this assumption is correct—then contact line depinning is highly undesirable. Its origin is unclear but probably depends on impurities.

An important property of the casted films is the relative absence of ring formation, due to the use of a solvent mixture. Figure 9 shows typical cross sections measured with the Dektak profiler. The sample in Figure 9A had a monomer/polymer mass ratio of 60:40% w/w. The sample in Figure 9B had a monomer/polymer mass ratio of 30:70% w/w. The degree of ring formation increases with polymer content, that is, the shape of the films depends on the solute composition; however, the middle of the films is usually flat. Grating shape and height were analyzed here. The leftmost and rightmost films are asymmetric in shape. Visual observation of the drying process reveals a "vapor pressure" of drying neighboring films, which deforms the sessile droplet, since the four droplets were deposited almost simultaneously. Both the leftmost and rightmost films experience an uncompensated pressure from the right and from the left, respectively, resulting in asymmetry.

It is seen that there is some thickness variation between different films. The methodology can certainly be improved

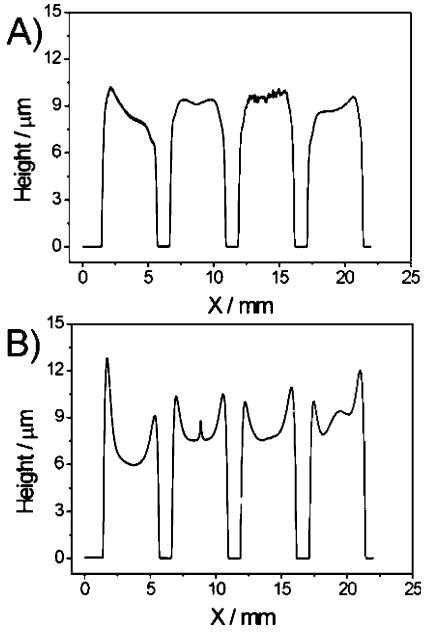

Figure 9. Cross sections of drop-casted films. (A) Monomer/polymer mass ratio 60:40% w/w. (B) Monomer/polymer mass ratio 30/70% w/w. A 3-μL portion of sample was deposited per film.

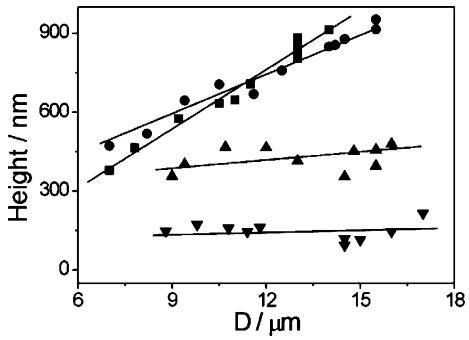

Figure 10. Grating height of film thickness (D)−grating period library. Grating period: ■, 40; ●, 20; ▲, 10; and ▼, 5 μm. Lines are drawn to guide the eye.

at this point, that is, drying the samples under a controlled atmosphere instead of ambient conditions; however, we are confident that the quality of the data is sufficient to recognize all important trends.

Film Thickness−Grating Period Library. A library with a discrete gradient in film thickness was prepared by dispensing onto a hydrophilic patch of the substrate various amounts of lacquer ranging from 3.0 to 13.0 μL in steps of 1.0 μL. The sample contained 5% w/w photoinitiator and had a monomer/polymer mass ratio of 1:1. Results are shown in Figure 10. The height of the 20- and the 40-μm period gratings increases approximately linearly with film thickness, whereas the 5- and 10-μm period gratings are virtually independent of thickness. Apparently, when the grating period exceeds the film thickness, influence of the latter on height is to be expected. An explanation for this phenomenon will probably involve the typical diffusion length of a monomer molecule relative to film thickness.

Photoinitiator Content−Grating Period Library. Eleven different samples were prepared. Their photoinitiator content ranges from 0 to 10 wt % in steps of 1%. The monomer to polymer mass ratio is 1:1. Three-microliter portions of solution were dispensed, yielding films with a thickness of 7 μm. Results are shown in Figure 11.

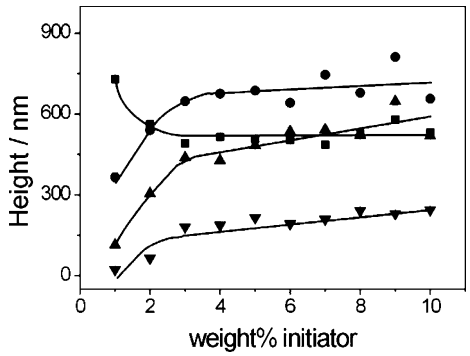

Figure 11. Grating height of photo initiator content−grating period library. Grating period: ■, 40; ●, 20; ▲, 10; and ▼, 5 μm. Lines are drawn to guide the eye.

This library closely resembles the energy dose−grating period library, because the concentration of radicals increases by increasing both energy dose and photoinitiator concentration. An important difference is the much larger grating height, which is probably related to the thickness of the films (7 versus 2.6 μm). In the range 1−3 wt % initiator, the height of the grating increases steeply with initiator concentration. At higher initiator concentration values, grating height increases much more slowly or stays constant. Only the 40-μm gratings behave differently: The height decreases with initiator concentration, similar to the decrease with increasing energy dose. The results can be explained in a similar way, that is, a high concentration of radicals leading to a high cross-linking density that hinders monomer diffusion to the central area (overexposure).

Monomer/Binder−Grating Period Library. Eleven different samples were tested. The monomer-to-polymer mass ratio varied from 70:30 to 20:80% w/w in steps of 5%. The photoinitiator content was 5 wt %. To prepare films, 3 μL of solution was dispensed, giving rise to a film thickness of 7 μm. Before polymerization, the samples with a monomer content of 60 wt % or more were tacky and turbid. The relief structure was already partially developed at room temperature, before the thermal development step. For applications, both effects are undesirable, because the lacquer becomes unsuitable for contact masking and for generation of complex structures through multiple exposure steps.

Results are shown in Figure 12. The height of the gratings generally increases with monomer concentration. Below 45 wt % monomer, the height increases linearly with concentration. Above 45 wt % monomer, the height increases more strongly. Above 60 wt % monomer, a plateau value is reached. This can be understood within the framework of the diffusion−polymerization model, as follows. The height generally increases with monomer concentration because more material becomes available to form a grating, whereas the concentration of polymer that hinders the diffusion of monomer decreases.

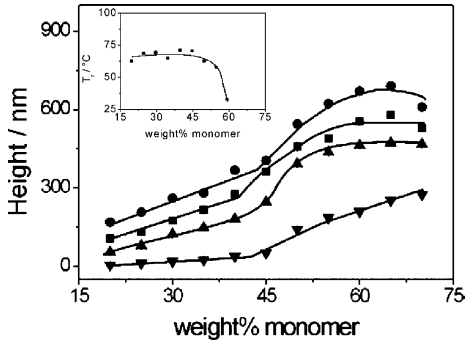

Figure 12. Grating height of monomer content−grating period library. Grating period: ■, 40; ●, 20; ▲, 10; and ▼, 5 μm. Lines are drawn to guide the eye. Inset: Onset of polymerization reaction, T_r, versus monomer content as determined from DSC trace. Above 55 wt % monomer, T_r suddenly drops to room temperature. The line is drawn to guide the eye.

Results of thermal analysis of the samples are shown in the inset of Figure 12. The onset of the exothermal peaks corresponding to the polymerization reaction, T_r, is approximately constant up to 50 wt % monomer, then decreases. At 60 wt % monomer, T_r suddenly drops to room temperature. Reaction takes place during the irradiation before heating, showing that monomer mobility is high in these blends at room temperature. Actually, the turbidity of the samples indicates phase separation. Microscopic observation of a phase-separated sample containing 65 wt % monomer that was annealed for 10 min at 80 °C clearly shows an internal structure of droplets embedded in a matrix. The drop in T_r and the observation of the relief structure already being partially developed at room temperature prove that this matrix consists of a low-viscosity compound, that is, the monomer.

Conclusions

Methodologies for the systematic and rapid investigation and optimization of photopolymer lacquers for photoembossing applications in terms of composition and processing parameters were developed. Continuous gradient libraries were prepared with a gradient in grating period along the short axis, and along the long axis, a gradient in exposure energy, using a gray scale mask, and a gradient in development temperature, using a temperature gradient heating stage. Discrete gradient libraries consisting of arrays of rectangular films were also prepared by dispensing a certain amount of sample on a chemically patterned substrate consisting of hydrophilic patches surrounded by hydrophobic, fluorinated barriers. Libraries with a discrete gradient in film thickness (through variation of the amount of sample), photoinitiator concentration, or monomer-to-polymer mass ratio were prepared. Uniformity of the film thickness after drying is controlled through the use of solvent pairs. Further improvement is expected by controlling the drying conditions. The methodology does not depend on any specific properties and can, therefore, be applied to other (coating) systems as well.

The topography of the photoembossed gratings was measured using an automated AFM. It allowed us to characterize one entire library of 44 samples within 9 h without human intervention. We analyzed the AFM results in terms of grating height and shape and arrived at the following set of conclusions: Largest heights are usually obtained at intermediate exposure energies. This optimum energy is larger for the smaller periods. Smaller gratings (5−10 μm) result in smaller heights due to surface tension effects. In the case of larger gratings (40 μm) overexposure results in a nonsinusoidal shape (low *S* factor) of the grating and height reduction. The effects of higher exposure energy and a higher initiator concentration are qualitatively very similar.

Grating height and shape gets more rounded with development temperature. This is due to the increased mobility of the monomer. However, at too high a temperature, the increased mobility of the photoinitiator causes the height to decrease, in particular, in the case of a 5-μm grating. For all other gratings, 100−120 °C seems to be an optimum range.

In the case of the 20- and 40-μm gratings, the height continuously increases with thickness. In the case of the 5- and 10-μm gratings, it is constant. Finally, the grating height increases with monomer concentration; however, above 55 wt % monomer, the reaction temperature suddenly drops to room temperature due to phase separation of the monomer/polymer mixture. In applications, this should be avoided.

Finally, we have demonstrated the power of a combinatorial methodology to improve the understanding of a complex process. We have also shown its power to optimize the height and shape of structures that are of great relevance for numerous applications.

Acknowledgment. The financial support of the Dutch Polymer Institute (DPI) and the Fonds der Chemischen Industrie is gratefully acknowledged.

References and Notes

(1) Meredith, J. C.; Karim, A.; Amis, E. J. *Macromolecules* **2000**, *33*, 5760.
(2) Meredith, J. C.; Smith, A. P.; Karim, A.; Amis, E. J. *Macromolecules* **2000**, *33*, 9747.
(3) Smith, A. P.; Sehgal, A.; Douglas, J. F.; Karim, A.; Amis, E. J. *Macromol. Rapid Commun.* **2003**, *24*, 131.
(4) Chattopadhyay, S.; Meredith, J. C. *Macromol. Rapid Commun.* **2004**, *25*, 275.
(5) Thelakkat, M.; Schmitz, C.; Neuber, C.; Schmidt, H.-W. *Macromol. Rapid Commun.* **2004**, *25*, 204.
(6) Deegan, R. D.; Bakajin, O.; Dupont, T. F.; Huber, G.; Nagel, S. R.; Witten, T. A. *Nature* **1997**, *389*, 827.
(7) Akhave, J. R.; Saunders: D.; Potyrailo, R. A.; Olson, D. R.; Flanagan, W. F. WO Patent 01/32320 A1, 2001.
(8) Grunlan, J. C.; Holguin, D. L.; Chuang, H.-K.; Perez, I.; Chavira, A.; Quilatan, R.; Akhave, J.; Mehrabi, A. R. *Macromol. Rapid Commun.* **2004**, *25*, 286.
(9) Tekin, E.; De Gans, B.-J.; Schubert, U. S. *J. Mater. Chem.* **2004**, *14*, 2627.
(10) Tekin, E.; Holder, E.; Marin, V.; De Gans, B.-J.; Schubert, U. S. *Macromol. Rapid Commun.* **2005**, *26*, 293.
(11) Boussie, T.; Devenney, M. U.S. Patent 2003129768 A1, 2003.
(12) Boussie, T.; Devenney, M. European Patent 1160262 A1, 2001.
(13) Croutxé-Barghorn, C.; Lougnot, D. J. *Pure Appl. Opt.* **1996**, *5*, 811.
(14) Sakhno, O.; Smirnova, T. *Optik* **2002**, *113*, 130.

(15) Witz, C.; Sánchez, C.; Bastiaansen, C. W. M.; Broer, D. J. In *Handbook of Polymer Reaction Engineering;* Meyer, T., Keurentjes, J., Eds.; Wiley-VCH: Weinheim 2005, Chapter19.
(16) DeWitz, C.; Broer, D. J. *Polym. Preprint* **2003**, *44*, 236.
(17) Suh, K. Y.; Seong, J.; Khademhosseini, A.; Laibinis, P. E.; Langer, R. *Biomaterials* **2004**, *25*, 557.
(18) Ghosh, P.; Amirpour, M. L.; Lackowski, W. M.; Pishko, M. V.; Crooks, R. M. *Angew. Chem., Int. Ed.* **1999**, *38*, 1592.
(19) Kim, C.; Burrows, P. E.; Forrest, S. R. *Science* **2000**, *288*, 831.
(20) Schueller, O. J. A.; Duffy, D. C.; Rogers, J. A. *Sens. Actuators, A* **1999**, *78*, 149.
(21) Adams, N.; de Gans, B,-J.; Kozodaev, D.; Sánchez, C.; Bastiaansen, C. W. M.; Broer, D. J.; Schubert, U. S. *J. Comb. Chem.*, in press.
(22) Sánchez, C.; de Gans, B.-J.; Kozodaev, D.; Alexeev, A.; Escuti, M. J.; van Heesch, C.; Bel, T.; Schubert, U. S.; Bastiaansen, C. W. M.; Broer, D. J. *Adv. Mater.* **2005**, *17*, 2567.
(23) Trimbach, D.; Feldman, K.; Spencer, N. D.; Broer, D. J.; Bastiaansen, C. W. M. *Langmuir* **2003**, *29*, 10957.
(24) Bex, P.; Makous, W. *J. Opt. Soc. Am. A* **2002**, *19*, 1096.
(25) Leewis, C. M.; De Jong, A. M.; Van IJzendoorn, L. J.; Broer, D. J. *J. Appl. Phys.* **2004**, *95*, 4125.
(26) Leewis, C. M.; De Jong, A. M.; Van IJzendoorn, L. J.; Broer, D. J. *J. Appl. Phys.* **2004**, *95*, 8352.
(27) Leewis, C. M. Ph.D. Thesis, Eindhoven University of Technology, Eindhoven, 2003.

CC0500506